Journal of Medical Sciences

ISSN 1682-4474

science alert

ANSInet
an open access publisher
http://ansinet.com

Research Paper

J. Med. Sci., 14 (3): 108-122
1st April, 2014
DOI: 10.3923/jms.2014.108.122

Brain Images Application and Supervised Learning Algorithms: A Review

[1]Baher H. Nayef, [1]Siti Norul Huda Sheikh Abdullah, [2]Rizuana Iqbal Hussain, [1]Shahnorbanun Sahran and [1]Abdullah H. Almasri

Medical image processing and classification are important in medicine. Many Magnetic Resonance Images (MRI) are taken for an individual. To reduce the radiologist workload and to enable more efficiency in brain tumor detection and classification. Many Computer Aided Diagnose (CAD) systems have been developed using different segmentation methods and classification algorithms. This study synthesizes and discusses some studies and their results. A Learning Vector Quantization (LVQ) classifier is used to classify MRI images into normal and abnormal. An initial experiment consisting of normal and abnormal MRI Brain Tumor dataset from UKM Medical Center, to observe various versions of LVQ classifiers performance is conducted. From the extensive and informative studies and numerical experiments, it is expected to obtain better brain tumor classification in the future using Multi pass LVQ classifier which obtained the least standard deviation value (0.4) and the mean accuracy rate is equal to 91%.

Key words: Brain imaging, segmentation, classification, learning vector quantization

JMS (ISSN 1682-4474) is an International, peer-reviewed scientific journal that publishes original article in experimental & clinical medicine and related disciplines such as molecular biology, biochemistry, genetics, biophysics, bio-and medical technology. JMS is issued eight times per year on paper and in electronic format.

For further information about this article or if you need reprints, please contact:

Siti Norul Huda Sheikh Abdullah
Pattern Recognition Research Group,
Center for Artificial Intelligence Technology,
Faculty of Information Science and Technology,
Universiti Kebangsaan Malaysia,
43600, Bangi, Selangor, Malaysia

Tel: +603-89216090/6183

ANSInet
Asian Network for Scientific Information

[1]Pattern Recognition Research Group, Center for Artificial Intelligence Technology, Faculty of Information System and Technology, Universiti Kebangsaan Malaysia, Malyasia
[2]Department of Radiology, UKM Medical Center, Universiti Kebangsaan Malaysia, 56000, Cheras, Kuala Lumpur, Malaysia

INTRODUCTION

Analysis the brain Magnetic Resonance Images (MRI) is a critical task. An accurate analyzing leads to early brain tumor detection. This enables the therapist to decide the suitable treatment. To help the radiologist to analyze the increasing number of MRI, a computer aided diagnoses (CAD) system has been developed. The CAD system output is not the final decision, but it provides as a second opinion for the radiologist to analyze the information faster, more accurately and less tiring than analyzing the images manually (Rajendran and Madheswaran, 2009).

Image segmentation is used to distinguish a normal image from the given images. Medical image segmentation is a helpful method for analyzing MRI or CT scan images. Segmenting MRI or CT scan images makes extracting abnormal features from any image easy and the differences are easily detected by comparing segmented images with known normal image features (Gaikwad *et al*., 2011). However, previous and current research in medical imaging has tended to focus on segmentation rather than classification.

Medical imaging can be defined as the technologies used to examine the human body to diagnose, monitor and treat medical conditions. Brain tumor imaging techniques are various such as CT, X-ray, Digital X-ray (DR), Digital Subtraction Angiography (DSA) (USFDA, 2012), Positron Emission Tomography (PET), Single Photon Emission Tomography (SPET), Fluorodeoxyglucose (FDG)-PET and Magnetic Resonance Imaging (MRI) techniques (Mingkun *et al*., 2011).

In this study MRI is the discussed technique. MRI is usually used to detect and visualize brain tumors. An MRI scanner (Hoffman, 2001; Coyne, 2012) provides detailed information about normal and abnormal brain tissues as shown in Fig. 1a and 2, respectively. To obtain better delineation in some cases, a contrast material is given to the patient either orally or as an injection (USFDA, 2012). To differentiate tissue types according to

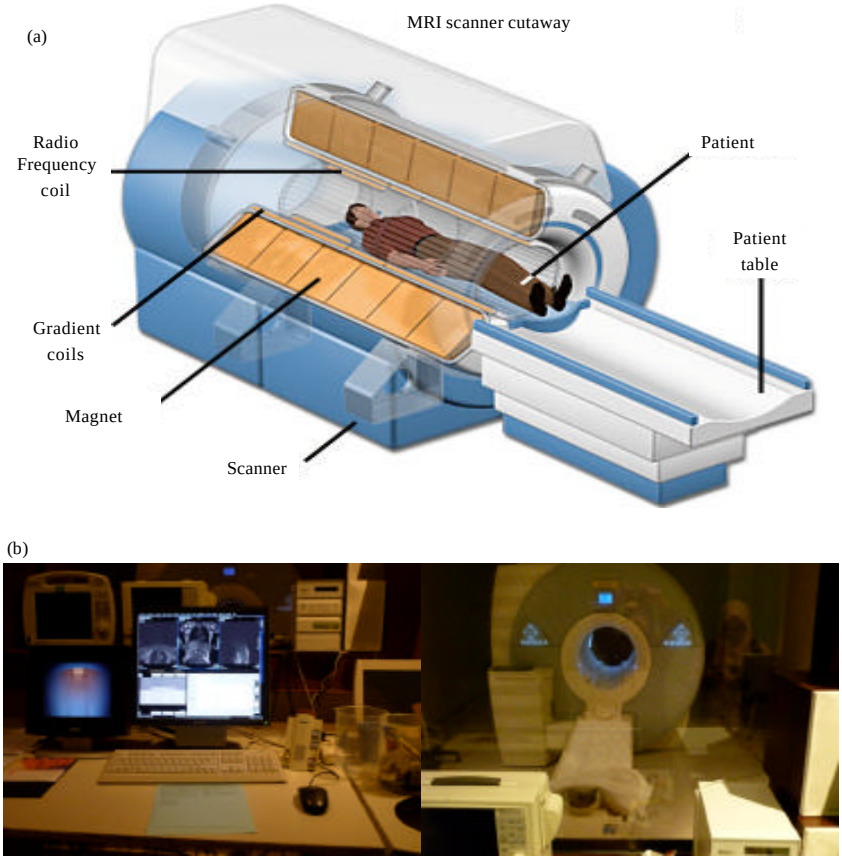

Fig. 1(a-b): (a) MRI scanner (Source: Coyne, 2012) and (b) UKM Medical Center, Malaysia

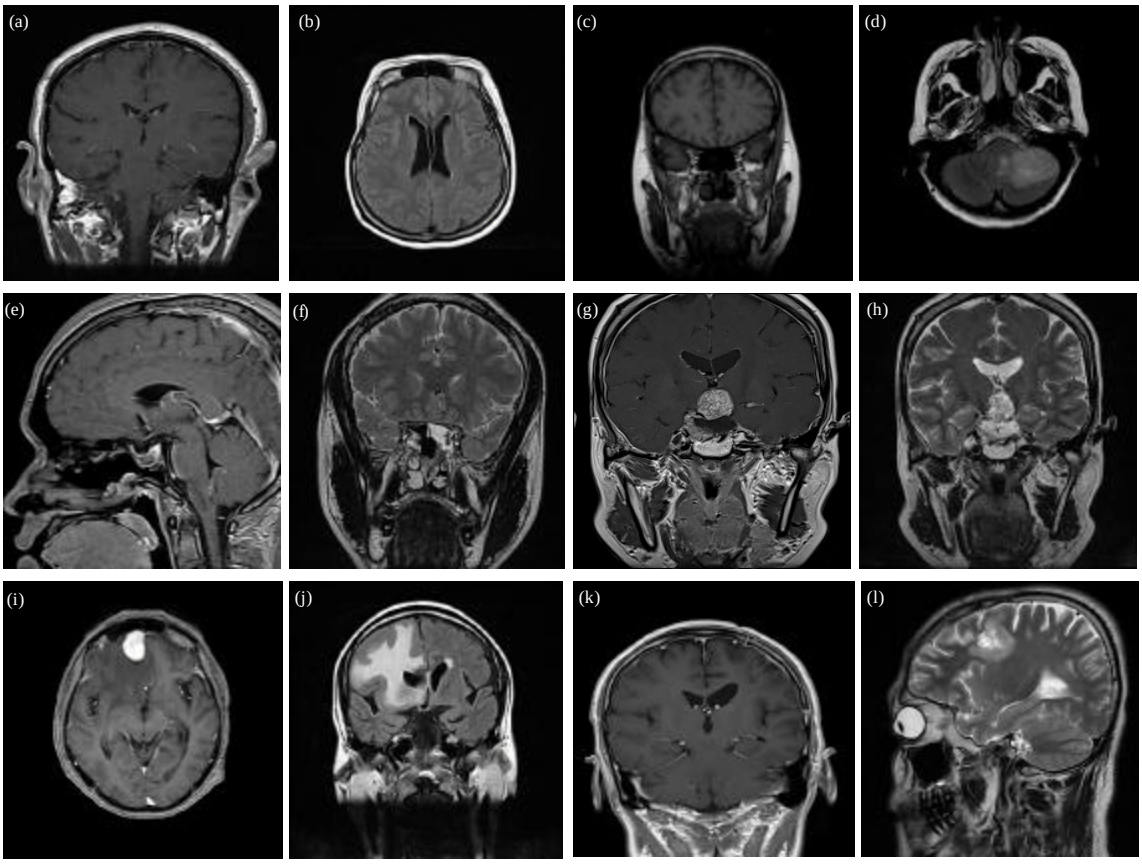

Fig. 2(a-l): Examples of axial sequences in (a-b) Normal and (c-l) Abnormal brain MRI image. (a) Normal, (b) T1-axial at Sequence 9, T2-axial at sequence 14, (c) Grade 1 meningothelial meningioma, (d) T1-axial at sequence 15 T2: T2-axial at sequence (15), (e) Grade 1 pituitary adenoma, (f) T1-axial at sequence 59 T2-axial at sequence 1, (g) Grade 2 diffuse astrocytoma, (h) T2-axial at sequence 8, T2-axial at sequence 10, (i) Grade 3 rhabdoid meningioma, (j) T1-axial at sequence 8 T2-axial at sequence 9, (k) Grade 4 medulloblastoma T1-axial at sequence 9, (l) T2-axial at sequence 13. (1) T1_axial (2) T2_axial. Source: Collected data from UKM Medical Center, Malaysia

the proton density in MRI, T1 and T2 relaxation times are used. To achieve a particular weighting in T1 and T2, a special pre-pulse must be applied to discriminate between water and fat (Kirsch *et al*., 2009). The medical imaging techniques can be further enhanced by injecting the intelligent computing techniques for diagnostic sciences in biomedical image classification.

Malignant tumors contain cancer cells which spread to the surrounding brain tissues, grow quickly and are life threatening. There are I-IV grades of primary tumors and the grade of a tumor depends on the appearance of the cells under the microscope (NCI, 2009). The second type of brain tumor is called metastatic which refers to a cancer that begins in another part of the body and spread to the brain. Metastatic tumors can be classified according to the position of the tumor in the brain, the type of the tissue from which it originated, or the original location (MedlinePlus, 2012).

Numerous studies have been conducted on brain MRI images (Sasikala*et al*., 2006; Chalabi *et al*., 2008; Shubhangi and Hiremath, 2009; Gopal and Karnan, 2010; Cherifi *et al*., 2011; Lahmiri and Boukadoum, 2011; Abdullah *et al*., 2011).

Sasikala *et al*. (2006) discussed segmenting the Glioblastoma-Multiforme tumor from brain MR images. They used the special Gray level dependence (SGLDM) and wavelet transform methods to extract texture features and classify the ROI from the brain tissues into normal and abnormal (tumor). They applied a Genetic

Algorithm (GA) to find the optimal texture features, minimized the number of features and increased Artificial Neural Network (ANN) classifier accuracy. They also used three segmentation methods: Optimal Feature based-segmentation, tumor segmentation using region growing and tumor region segmentation using a fuzzy c-means algorithm. The results showed that their proposed method outperformed the other two methods.

Chalabi *et al.* (2008) applied three classification algorithms, SOM, LVQ and a combination of SOM and LVQ, to classify the MR images. They used a manual selection technique to segment the MRI into gray and white substances by taking samples that represent normal and abnormal areas. The results of these three algorithms are compared according to the QE (Quantization Error) and CR (Classification Rate).

Shubhangi and Hiremath (2009) proposed a real time design to detect brain tumors from MR images. Their design combines knowledge-based techniques and a multi-spectral analysis based on a Support Vector Machine (SVM). Their approach showed good performance in detecting normal and abnormal tissues. The constructed system allowed repeated refinement to apply the unsupervised segmentation and classification decisions. They proposed a new process, called "knowledge-engineering", in which a set of heuristics rules were used to show the effects of applying variant pulse sequences on different types of brain tissues to decide which type of knowledge is the most useful for segmenting images.

Gopal and Karnan (2010) introduced a new approach to detect and diagnose brain tumors using a combination of Fuzzy C-Means (FCM) and intelligent optimization algorithms like (GA) and Particle Swarm Optimization (PSO). They first enhanced MR images using a tracking algorithm to remove film artifacts and a median filter to remove noise. To segment and classify MR images, they applied FCM with GA then FCM with POS. The results showed that the average accuracy of FCM with GA was 89% and the classification error rate was 0.078%; for the proposed method, FCM with POS accuracy was 92.8% and the classification error rate was 0.059%. The proposed method's execution time was longer than that of FCM with GA because POS processes images layer-by-layer and FCM uses clustering techniques.

Cherifi *et al.* (2011) applied two segmentation methods to MRI brain images for a specific area of the brain, the cerebrum and showed necrotizing tissues implanted within the anaplastic Glioblastoma Multiform (GBM) tissue cells. They filtered the images from noise using a median filter, then next applied local, global and Otsu thresholding to separate the tumor from the background. The second segmentation method used Expectation Maximization (EM) to extract tumors using characteristics, including the mean and the variations in pixel intensity. EM method showed better results in recognizing necrotizing tissues especially for detection small regions of necrotizing tissue.

Lahmiri and Boukadoum (2011) used wavelet decomposition of the MRI images, extracted features from Low High (LH) and High Low (HL) sub-bands using a first order statistic and classified images using a Support Vector Machine (SVM). The results were comparable to the method that extracted features using the LL sub-band. They explained that the features extracted from horizontal and the vertical sub-band was helpful and more computationally intensive for classifying the normal and abnormal image textures than the LL sub-band. In addition, they developed an ensemble of classifiers that combine k-NN, Perceptron Neural Network (PNN) and LVQ. The results collected from the ensemble classifiers outperformed the performance of these classifiers separately. However, in their study the ensemble classifiers showed high accuracy rate with normal images while considerable accuracy with abnormal images.

Abdullah *et al.* (2011) discussed brain MRI segmentation and classification. They preprocessed images to remove noise using two wavelet transform algorithms: Daubechies-4 (DAUB4) and Haar. For classification, they used the Support Vector Machine (SVM) algorithm. They used wavelet approximate coefficients as inputs for the SVM algorithm. The proposed approach did not achieve good classification accuracy, due to noise in the MR images and misclassified data.

Artificial intelligence techniques such as Neural Networks have been proven to give better classification accuracy as classification of image is an important step in CAD approach. Most research in medical image classification focuses on Neural Networks particularly emphasizing back propagation (RajaRajan, 2011). Further investigations are needed to evaluate other special Neural Network techniques; like LVQ which has a very simple architecture, it will be of most interest and will be discussed in the next subsections. The generalization ability is the main advantage of the LVQ classifier (Pregenzer and Pfurtscheller, 1995). It can create decision regions that are almost optimal (Khuwaja, 2002). This study designed to evaluate the LVQ algorithm for diagnostic science applications. The evaluation results provide a better framework for development of emerging medical systems, enabling the better delivery of healthcare particularly brain cancer.

Researchers have applied various examples of NN architecture to pattern recognition. Existing popular NN architectures are: Multi-Layer Perceptron (MLP), Radial Basis Function (RBF), Learning Vector Quantization (LVQ), Adaptive Resonance Theory (ART), Auto-Associative NNS and Kohonen Self-Organising

Maps (SOM). As with NN architecture, there are also many rules for NN learning. NN learning rule are commonly divide to two types which are supervised and unsupervised. This study focuses on supervised learning only. Classification accuracy is used as the performance criterion.

From the previous studies LVQ classifier showed its outstanding performance, this motivated the researchers to experiment its performance with the brain data set. Brain data set are collected from UKM (Universiti Kebangsaan Malaysia) Medical Center.

MATERIALS AND METHODS

In this section it is explained how image acquisition method used in this study, the history and theoretical of LVQ. The initial proposed framework of Brain MRI classification based on filtering, Morphological and segmentation methods for preprocessing phase and Grey Level Co-occurrence Matrix (GLCM) method as the input features and LVQ methods are for post-processing phase are all explained.

Image acquisition: The images are captured by the radiologist from UKM (Universiti Kebangsaan Malaysia) Medical Center. The sample of MRI Scannet Cutaway and MRI Scanner at Department of Radiologist, UKM Medical Center are in Fig. 1b, respectively.

The collected dataset consists of 148 abnormal and 52 normal MRIs from 10 patients. MRI scanner produces sagittal, coronal andaxial sequences. In this study, only T1 and T2 weighted axial sequence are used in Fig. 2. For each Brain tumor patient, about 5 to 6 images for different slices were selected.

For training and testing, percentage splitting dataset is applied. The datasets are split into training and testing datasets using split percentage method (holdout method). The used splits are 40, 45, 50, 55, 60, 65, 67, 70, 75 and 80. This study follows the same procedure of splitting percentage method as Haralick *et al.* (1973). For example if the splitting dataset is 40, therefore, 40% of the whole dataset as in the Table 1 and 2 is used as training dataset while the remain is set as the testing dataset. The dataset is selected based on random sampling. The experiment is conducted using this split percentage method and evaluate the LVQ network based on accuracy performance after testing on MRI brain images Table 1 and benchmark datasets namely UCI Segmented challenge and UCI Segmented Test as the experiment control Table 2.

LVQ network in general: The LVQ neural network is a supervised version of the Self Organizing Map (SOM) algorithm, introduced by Kohonen (1988) as a modified Labeled Vector Quantization. The LVQ neural network works by approximating the class distribution using the

Table 1: UKM Medical Center axial sequence brain tumor images

Dataset name	No. of instances	Spatial resolution	No. of features	No. of classes	Source
(a)					
Brain tumor images	200	320×320	21	2 (Normal, Abnormal)	UKM Medical Center
Class type		T1 sub total	T2 sub total		
Normal		34	18		
Abnormal		118	30		
Abnormal sub-class type		Cancerous type	No. of patient data	Range of tumor size based on medical expert report	
(b)					
Abnormal (grade 1)		Craniopharyngioma	1	1.0 cm(AP)×1.1 cm(W)×1.0 cm(CC)	
		Meningothelial meningioma	1	0.5 cm(AP)×0.7 cm(W)×0.6 cm(CC)	
		Diffuse large B-cell lymphoma	1	2.8 cm(AP)×3.8 cm(W)×3.8 cm(CC)	
		Pituitary adenoma	4	1. Missing measurement value 2. Missing measurement value 3. 1.28 cm(AP)×1.4 cm(W)×1.2 cm(CC) 4. 0.8 cm(AP)×0.7 cm(W) × 0.8 cm(CC)	
Abnormal (grade 2)		Diffuse astrocytoma	1	No evidence of tumour recurrence	
Abnormal (grade 3)		Rhabdoid meningioma	1	3 cm	
Abnormal (grade 4)		Medulloblastoma	1	1.0 cm(AP)×3.0 cm(W) × 2.2 cm(CC)	

Dataset 1 (a) General and (b) Specific. Source: Collected data from UKM Medical Center Malaysia

Table 2: UCI segmented challenge and segment-test dataset

Dataset name	No. of Instances	No. of features	No. of Classes
Segmented challenge	1500	(19) region centroid col, region centroid row, region pixel count, short line density 5, short line density 2, vedge mean, vegde sd, hedge mean, hedge sd, intensity mean, rawred mean, rawblue mean, rawgreen mean, exred mean, exblue mean, exgreen mean, value mean, saturatoin mean, hue mean	7 (brickface, sky, foliage, cement, window, path and grass)
Segmented test	810		

Source: (Bache and Lichman, 2013)

minimum number of codebook vectors that will reduce errors in the classification phase. The LVQ algorithm learns to classify the input vectors according to predefined classes. Subsets of identical codebook vectors are gathered into each class (Kohonen, 1988). Learning Vector Quantization (LVQ) networks are known good neural classifiers which provide fast and accurate results for many applications. LVQ is a widely used approach to classification. It is applied in a variety of practical problem areas including medical image and data analysis, for example in speech recognition and control chart pattern recognition. Classes are predefined and the data are labeled. The goal is to determine a set of prototypes that best represent each class. In vector quantization, it is assumed that there is a codebook which is defined by a set of M prototype vectors. (M is chosen by the user and the initial prototype vectors are chosen arbitrarily).

An LVQ network comprises three layers of neurons: An input buffer layer, a hidden layer and an output layer. The input layer carries out no information processing and only conveys the input patterns to the network. The hidden layer (also known as the Kohonen layer) performs actual information processing. The output layer yields the category of the input pattern. The network is fully connected between the input and hidden layers and partially connected between the hidden and output layers. Each output neuron is linked to a different cluster of hidden neurons. The hidden layers to output layer connections have their values fixed to 1. The weights of the connections between the input and hidden layers constitute the components of the reference vectors (one reference vector is assigned to each hidden neuron).

The reference vectors values are modified during the training of the network. Both the hidden neurons and the output neurons have binary outputs. When a Kohonen neuron wins the competition, it is turned 'on' (its activation value is made equal to 1) while others are automatically switched 'off' (their activation values are set to 0). This, in turn, makes the output neuron connected to the activated Kohonen neuron or to the cluster of hidden neurons that contains the winning neuron switch 'on' (emits a '1') and the rest switch 'off' (emits a '0'). The output neuron that produces a '1' gives the class of the input pattern. Each output neuron is dedicated to a different class.

LVQ algorithm: LVQ, as its name indicates, is based on vector quantization which is the mapping of an n-dimensional vector into one belonging to a finite set of representative vectors. That is, vector quantisation involves clustering input samples around a predetermined number of reference vectors. Learning in an LVQ network consists essentially of finding those reference vectors. The classification of input values into clusters is conducted on the basis of nearest neighbourhood and the smallest distance between the input vector and reference vectors is sought (smallest in the sense of the normal Euclidean distance). For each training pattern, the reference vector that is closest to it is determined. The corresponding output neuron is also called the winner neuron. At each learning iteration, the network is triggered only if its output is correct or incorrect and only the reference of that neuron which wins the competition by being closest to the input vector is activated and allowed to modify its connection weights. This movement of the reference vector is controlled by a parameter called the learning rate. It states how far the reference vector is moved as a fraction of the distance to the training pattern. Usually the learning rate is decreased in the course of time, so that initial changes are larger than changes made in later epochs of the training process. A simple LVQ training procedure is as follows (Xing and Pham, 1995):

- Initialise the weights of the reference vectors
- Present a training input pattern to the network
- Calculate the (Euclidean) distance between the input pattern and each reference vector
- Update the weight of the reference vector of the winning hidden neuron that is closest to the input pattern. If the input pattern belongs to the cluster connected to the output neuron class, the reference vector is moved closer to the input pattern. Otherwise, the reference vector is moved away from the input pattern
- Return to (ii) with a new training input pattern and repeat the procedure until all training patterns are correctly classified (or a stopping criterion is met)

The LVQ procedure is translated into flow chart of a standard LVQ network steps as shown in Fig. 3.

Structure of the network: LVQ network consists of one input layer, Hidden or Kohonen Layer (competitive layer) with full connection between them and one output layer with partial connection with Kohonen layer as shown in Fig. 4. The input layer contains 21 neurons (equal to the No. of attributes), the competitive layer contains 40 neurons (40 codebook vectors). Number of code vectors per class depends on the class distribution proportion.

Learning procedure in standard LVQ networks: Good performance in an LVQ network depends on the correct number of reference vectors being assigned to each category, their initial values and the choice of a proper learning rate and stopping criterion. In general, the Euclidean distance is adopted as a basic rule of competition between the weight vectors of the reference vectors and the GLCM input vector. The distance d_i between the weight vectors W_i of neuron I and the GLCM input vector X is given by:

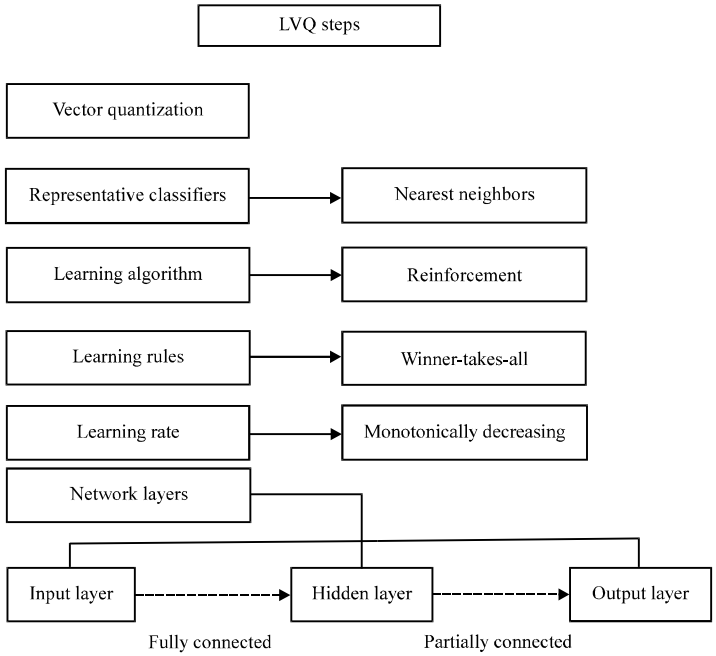

Fig. 3: Steps of a standard LVQ network. (Source: Xing and Pham, 1995)

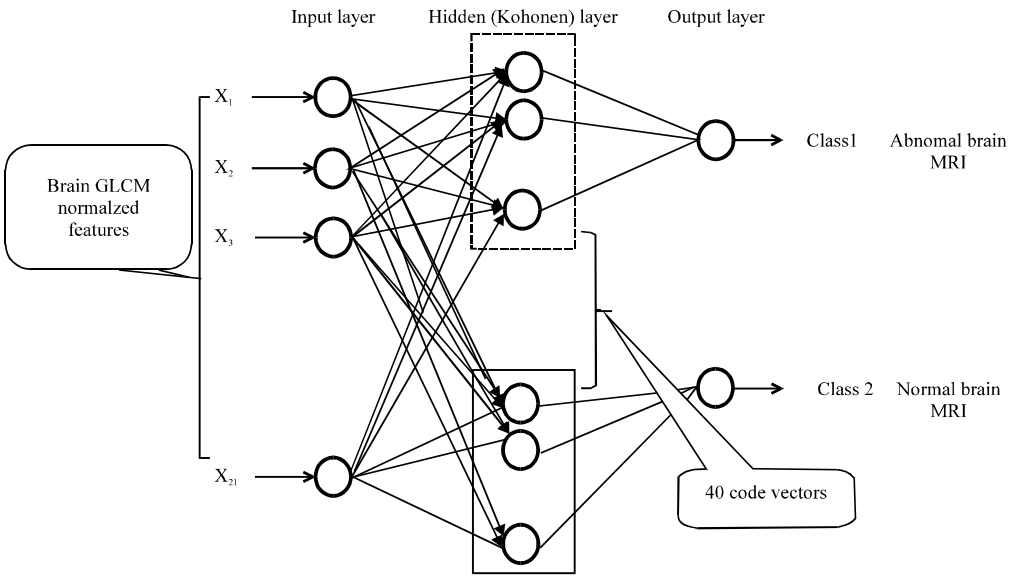

Fig. 4: Proposed LVQ structure based on GLCM features

$$d_i = \|W_i - X\| = \sqrt{\Sigma_j (W_{ij} - X_j)^2)} \quad (1)$$

where, W_{ij} and X_j are the jth GLCM components of W_i and X, respectively. The neuron which has the minimum distance wins the competition and is permitted to change its connection weights in each learning iteration. The learning formula for updating the reference vector is given as follows.

If the winning neuron is in the correct category, then:

$$W_{new} = W_{old} + \lambda(X - W_{old}) \quad (2)$$

And if the winning neuron is in the incorrect category, then:

$$W_{new} = W_{old} - \lambda(X - W_{old}) \quad (3)$$

In Eq. 2 and 3, λ is the learning rate (usually, $0<\lambda<1$) which decreases monotonically with the number of iterations. The implication of the learning rule expressed in Eq. 2 and 3 is that the weight or reference vector is updated to be close to the input vector if it represents the input pattern and is pushed away if it does not.

LVQ network configuration: It consists of one input layer, on competitive layer (hidden) and one output layer. The initial parameters of LVQ classifiers such as number of iterations, learning rate and the codebook vectors were selected based on different runs. Thus, the selected initial parameters of LVQ series are 1000, 0.3, 40, respectively.

Brain MRI segmentation and classification proposed framework: This proposed framework shows the overall procedure where the LVQ classifier is applied, the proposed framework contains two phases: Preprocessing and post-processing as shown in Fig. 5.

In the preprocessing, data preprocessing techniques was applied to enhance the images and extract texture features. Image enhancement includes applying two types of filters. The first is high pass filter which consists of fourier transform, butterfly and exponential high pass filtering processes for sharping the edges in the respective image and the second is Median filter. It is used due to its excellence noise reduction capability with considerably less blurring than linear smoothing filters of similar size.

Next step is applying watershed and Otsu (1979) segmentation techniques and convert the images into binary form. Closing and Opening morphological operations were applied to extract pixels with the highest intensities which represent the tumor region then combined the tumor region image with the original image. Gray Level Co-occurrence Matrix (GLCM) (Haralick *et al*., 1973; Soh and Tsatsoulis, 1999; Clausi, 2002; Bataineh *et al*., 2012) was used to extract the texture features of the final images as shown in Fig. 6. The extracted features are listed in Table 3.

Next step was testing LVQ series such as Hierarchy LVQ, LVQ1, LVQ2.1, LVQ3, Multi-pass LVQ, OLVQ1 and OLVQ3 to classify the output of the segmented images into normal and abnormal.

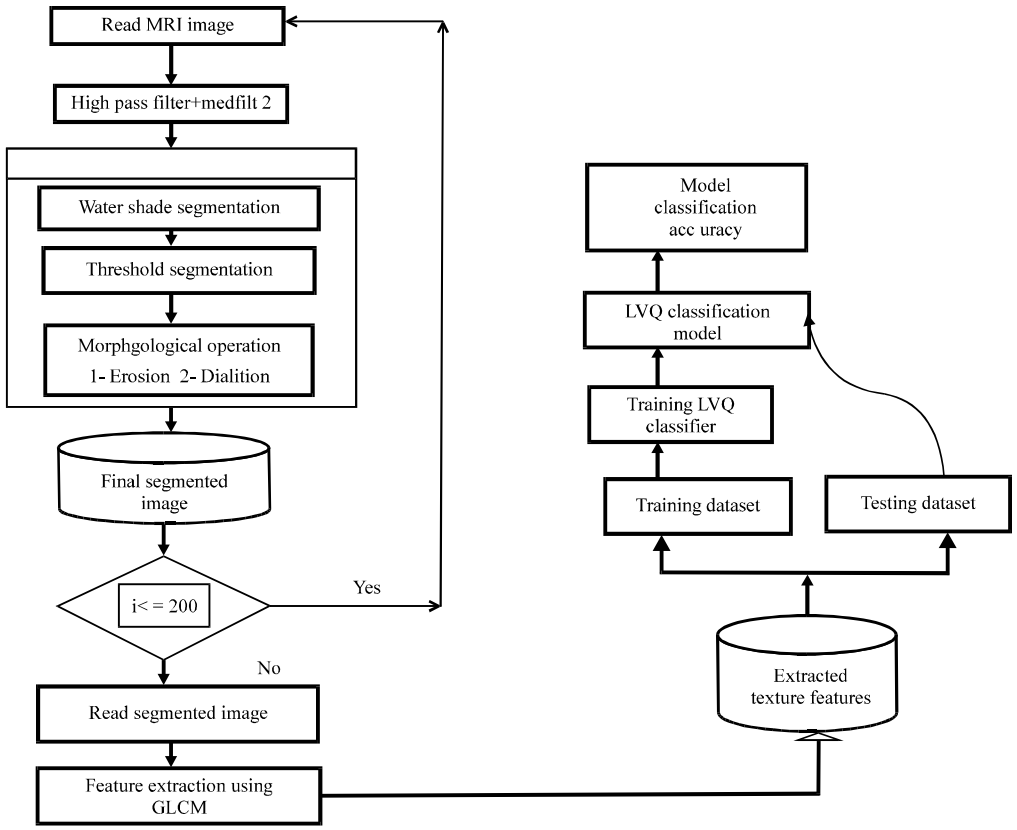

Fig. 5: Proposed framework for brain MRI classification

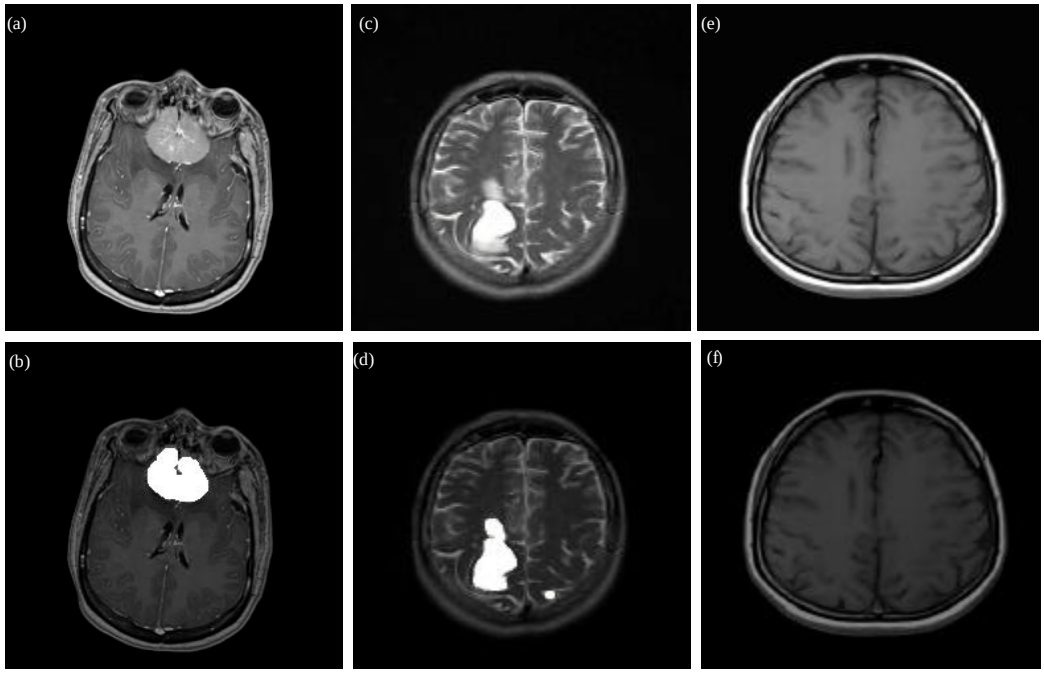

Fig. 6(a-f): Images before segmentation for abnormal cases (a) T1 sequence 25 and (c) T1 sequence 13 and normal case (e) T1 sequence 1 and (b, d and f) are output images after segmentation phase. Source: Collected data from UKM Medical Center, Malaysia

Table 3: Gray level co-occurrence matrix (GLCM) features

Attribute	Source
Autocorrelation	Haralick *et al.* (1973)
Correlation	Haralick *et al.* (1973) and Soh and Tsatsoulis (1999)
Cluster prominence	Haralick *et al.* (1973)
Cluster shade	Haralick *et al.* 1973)
Dissimilarity	Haralick *et al.* (1973)
Energy	Haralick *et al.* (1973)
Entropy	Haralick *et al.* (1973)
Contrast	Haralick *et al.* (1973) and Soh and Tsatsoulis (1999)
Homogeneity	Haralick *et al.* (1973)
Maximum probability	Soh and Tsatsoulis (1999)
Sum of squares variance	Haralick *et al.* (1973)
Sum average	Haralick *et al.* (1973)
Sum variance	Haralick *et al.* (1973)
Sum entropy	Haralick *et al.* (1973)
Difference variance	Haralick *et al.* (1973)
Difference entropy	Haralick *et al.* (1973)
Information measure of correlation1	Haralick *et al.* (1973)
Information measure of correlation2	Haralick *et al.* (1973)
Inverse difference normalized (INN)	Clausi (2002)
Inverse difference moment normalized	Clausi (2002)

RESULTS

The results of testing LVQ series with three data sets: The collected brain tumor dataset and two standard datasets from University of California (Bache and Lichman, 2013) which are segmented challenge and segment test datasets explained in Fig. 7.

The initial parameters used to run this experiment is 1000 for number of iteration, 0.3 learning rate, 40 codebook vectors and use voting = true. In LVQ2 classifier the allowed window size (w) of matching codebook vectors is 0.3. In LVQ3 classifier Epsilon learning weight (E = 0.1) modifier is used when both BMUs are of the same instances class.

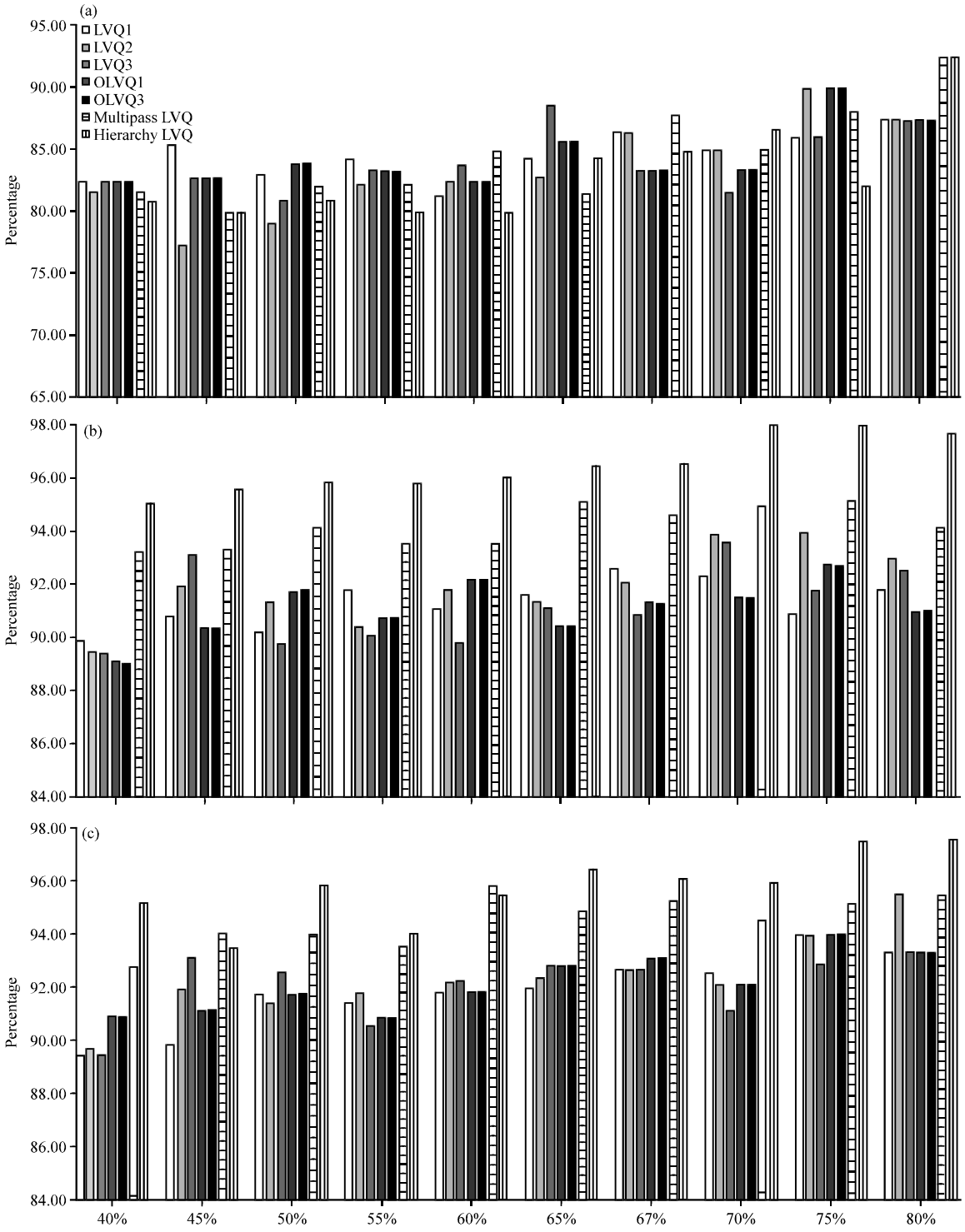

Fig. 7(a-c): Various LVQ classification accuracy rates in comparison to dataset split percentages using (a) UKM Medical Center MRI Brain Tumor Image dataset, (b) Segment-challenge dataset and (c) Segment-test dataset "No. of iteration = 1000, Learning Rates = 0.3"

The datasets are split into training and testing datasets using split percentage method (holdout method). The used splits are 40, 45, 50, 55, 60, 65, 67, 70, 75 and 80. This study follows the same procedure of splitting

Table 4: Accuracy rates of the MRI brain tumor image dataset

Split percentage	LVQ1 (%)	LVQ2 (%)	LVQ3 (%)	OLVQ1 (%)	OLVQ3 (%)	MultipassLVQ (%)	HierarchyLVQ (%)
40	82.50	81.67	82.50	82.50	82.50	81.67	80.83
45	85.45	77.27	82.73	82.73	82.73	80.00	80.00
50	83.00	79.00	81.00	84.00	84.00	82.00	81.00
55	84.44	82.22	83.33	83.33	83.33	82.22	80.00
60	81.25	82.50	83.75	82.50	82.50	85.00	80.00
65	84.29	82.86	88.57	85.71	85.71	81.43	84.29
67	86.36	86.36	83.33	83.33	83.33	87.88	84.85
70	85.00	85.00	81.67	83.33	83.33	85.00	86.67
75	86.00	90.00	86.00	90.00	90.00	88.00	82.00
80	87.50	87.50	87.50	87.50	87.50	92.50	92.50

"No of iteration =1000, Learning rates = 0.3"

Table 5: Accuracy rates of the segment-challenge dataset

Split percentage	LVQ1 (%)	LVQ2 (%)	LVQ3 (%)	OLVQ1 (%)	OLVQ3 (%)	Multipass LVQ (%)	HierarchyLVQ (%)
40	89.00	88.67	88.67	88.33	88.33	91.89	93.44
45	89.82	90.79	91.78	89.45	89.45	92.00	93.94
50	89.33	90.27	88.93	90.67	90.67	92.67	94.13
55	90.67	89.48	89.19	89.78	89.78	92.15	94.07
60	90.00	90.67	89.00	91.00	91.00	92.17	94.33
65	90.48	90.29	90.10	89.52	89.52	93.52	94.67
67	91.31	90.91	89.90	90.30	90.30	93.13	94.75
70	91.11	92.44	92.22	90.44	90.44	93.33	96.00
75	89.87	92.53	90.67	91.47	91.47	93.60	96.00
80	90.67	91.67	91.33	90.00	90.00	92.67	95.67

"No of iteration = 1000, Learning rates = 0.3"

percentage method as Haralick *et al.* (1973). The performance accuracy rates of all the LVQ classifiers with the brain tumor dataset are shown in Table 4. In overall, the split (75) shows better accuracy rates than the other splits and the highest accuracy rate belongs to LVQ2, OLVQ1 and OLVQ3 classifiers with accuracy rate (90%) while the other classifiers obtained as follow: LVQ1 is 86%, LVQ3 is 86%, Multipass LVQ is 88% andfinally Hierarchy LVQ is 82%.

Figure 7a explains the performance of LVQ serise with brain tumor dataset. The performance of LVQ1 is slightly better than OLVQ1 in splits (45, 55, 67 and 70) and at splits 50, 60, 65 and 75 OLVQ1 outperforms LVQ1 and the rest are equal. OLVQ3 outperforms LVQ3 at 50, 70 and 75 splits and LVQ3 outperform OLVQ3 at accept at 60 and 65 splits. Hirerarchy LVQ performance has been improved by increasing the split percentage. Multipass LVQ showed a stability in splits 40-60 and start to increase in splits 65-70. LVQ2 performance showed high accuracy in split 75 but for the rest of the splits the accuracy was low. In general all the versions of LVQ algorithms showed the best accuracy at split 75%.

The segmented challenge dataset consists of 1500 instances, 19 attributes and 7 classes. The LVQ classifiers accuracy rates with this dataset are shown in Table 5. The accuracy rates of most LVQ classifiers showed better results in split 75 than the other splits. The accuracy rate of LVQ1 classifier is 89.87%, LVQ2 is 92.53%, LVQ3 is 90.67%, OLVQ1 is 91.47%, OLVQ3 is 91.47%, Multi-Pass LVQ is 93.60 and for Hierarchy LVQ is 96% as shown in Table 5 and Fig. 7b.

The results of classifying segmented challenge dataset are shown in Fig. 7b. The Hierarchy LVQ classifier outperformed the rest of the classifiers with stable accuracies in all dataset splitting percentages. The other LVQ classifiers are slightly different. Similar to UKM Medical Center Brain Tumor's experimental results, the optimal dataset splitting percentages for all LVQ series is 75%.

The third standard dataset used in this study to test the performance of LVQ series is the segment-test dataset. It consists of 810 instances, 19 attributes and 7 classes. The classification accuracy rates are shown in Table 6 and Fig. 7c. In general the best split which shows the best accuracy rates for most of the LVQ classifiers is split 75. In this split the accuracy performance of LVQ1 is 92.61%, LVQ2 is 92.61%, LVQ3 is 91.63%, OLVQ1 is 92.61%, OLVQ3 is 92.61%, Multi-pass LVQ is 93.60% and for Hierarchy LVQ is 95.57%.

In addition to the brain tumor images, LVQ series are tested using second standard data sets from UCI the segment-challenge and segment-test datasets. The accuracies of all LVQ series are decreasing at 60% except for LVQ2, OLVQ3 and Multipass LVQ for brain tumor dataset, the accuracies of all LVQ series are decreasing at 55% except for LVQ1 and LVQ3 for

Table 6: Accuracy rates of the segment-test dataset

Split percentage (%)	LVQ1 (%)	LVQ2 (%)	LVQ3 (%)	OLVQ1 (%)	OLVQ3 (%)	Multipass LVQ (%)	Hierarchy LVQ (%)
40	88.68	88.89	88.68	89.92	89.92	91.56	93.62
45	89.01	90.36	89.24	90.13	90.13	92.60	92.15
50	90.62	90.37	91.36	90.62	90.62	92.59	94.07
55	90.41	90.68	89.59	89.86	89.86	91.78	92.60
60	90.74	91.05	91.05	90.74	90.74	94.14	93.83
65	90.85	91.20	91.55	91.55	91.55	93.31	94.72
67	91.42	91.42	91.42	91.79	91.79	93.66	94.40
70	91.36	90.95	90.12	90.95	90.95	93.00	94.24
75	92.61	92.61	91.63	92.61	92.61	93.60	95.57
80	91.98	93.83	91.98	91.98	91.98	93.83	95.68

No of iteration = 1000, Learning rates = 0.3

Table 7: Classification accuracy rates for all variations of LVQ using UKM Medical Center brain tumor dataset at its optimal split percentages

UKM medical center brain tumor

Split (%)	LVQ1 (%)	LVQ2 (%)	LVQ3 (%)	OLVQ1 (%)	OLVQ3 (%)	Multipass LVQ (%)	Hierarchy LVQ (%)
40							
Accuracy	82.50	81.67	82.50	82.50	82.50	81.67	80.83
Sensitivity	82.50	81.70	82.50	82.50	82.50	81.70	80.80
Specificity	61.50	53.90	59.80	61.50	61.50	61.30	73.60
45							
Accuracy	85.45	77.27	82.73	82.73	82.73	80.00	80.00
Sensitivity	85.50	77.30	82.70	82.70	82.70	80.00	80.00
Specificity	66.40	42.80	54.10	55.40	55.40	53.20	66.00
50							
Accuracy	83.00	79.00	81.00	84.00	84.00	82.00	81.00
Sensitivity	83.00	79.00	81.00	50.00	50.00	54.20	65.50
Specificity	56.00	63.00	63.80	93.60	93.60	90.80	87.30
55							
Accuracy	84.44	82.22	83.33	83.33	83.33	82.22	80.00
Sensitivity	84.40	82.20	83.30	83.30	83.30	82.20	80.00
Specificity	58.10	63.50	54.30	76.20	76.20	73.90	67.40
60							
Accuracy	81.25	82.50	83.75	82.50	82.50	85.00	80.00
Sensitivity	81.30	82.50	83.80	82.50	82.50	85.00	80.00
Specificity	67.10	48.00	47.80	50.80	50.80	66.30	66.70
65							
Accuracy	84.29	82.86	88.57	85.71	85.71	81.43	84.29
Sensitivity	84.30	82.90	88.60	85.70	85.70	81.40	84.30
Specificity	65.50	51.70	64.80	71.30	71.30	57.90	76.40
67							
Accuracy	86.36	86.36	83.33	83.33	83.33	87.88	84.85
Sensitivity	86.40	86.40	83.30	83.30	83.30	87.90	84.80
Specificity	59.80	63.60	53.80	52.20	52.20	74.90	87.80
70							
Accuracy	85.00	85.00	81.67	83.33	83.33	85.00	86.67
Sensitivity	85.00	85.00	81.70	83.30	83.30	85.00	86.70
Specificity	62.50	60.70	61.50	67.80	67.80	82.50	84.10
75							
Accuracy	86.00	90.00	86.00	90.00	90.00	88.00	82.00
Sensitivity	86.00	90.00	86.00	90.00	90.00	88.00	82.00
Specificity	79.60	77.60	68.40	89.10	89.10	67.00	73.70
80							
Accuracy	87.50	87.50	87.50	87.50	87.50	92.50	92.50
Sensitivity	87.50	87.50	87.50	87.50	87.50	92.50	92.50
Specificity	72.70	63.60	74.80	52.30	52.30	82.50	92.00

segment-challenge dataset and the accuracies of all LVQ series are decreasing at 55% except for LVQ2 for segment-test dataset. Then, a sudden rise is shown in all accuracy rate results for all LVQ series. As conclusion, this experiment has also proven the outperformance of the Hierarchy LVQ compared to the other algorithms for segment-challenge and segment-test dataset, the Multi-pass LVQ shows better performance than Hierarchy LVQ for Brain Tumor dataset as shown in Fig. 7.

The best dataset split percentages for each dataset is selected, as shown in Table 7. Multi-pass LVQ has produced the least standard error accuracy rates in comparison with all other LVQ series in all datasets. Thus,

Multi-pass LVQ is more stable than the other classifiers and has the potential to be improved in the future.

Based on True-Positive (TP), True-Negative (TN), False-Positive (FP) and False-Negative (FN) measures, statistical performance is calculated, such as sensitivity TP/TP+FN, specificity TN/TN+FP and accuracy TP+TN/TP+TN+FP+FN, respectively. Based on Table 7, sensitivity rate for the LVQ and its siblings are able to recognize abnormal images in the interval of 81.70-90%. This result showed at 70-75% splitting dataset. On the other hand, specificity rates which represents the true negative of normal image, falls in the interval of 60.7-89.10% at the same splitting dataset. In conclusion, overall performance showed that accuracy of the LVQ and its siblings are acceptable in the range of 81.67-90%. This has also determined the most suitable splitting dataset within 70-75%.

Finally, ANOVA statistic test was applied to confirm or reject the mean differences between all the classifiers. The null hypothesis H_o states that there is no significant difference in the performance accuracy rates of all LVQ series with the three datasets. For $\alpha = 0.05$ (the confidence level is (95%), the calculated p-value is equal to 0.42 which is greater than 0.05, the F value is equal to 1.078 which is less than F critical (2.8477). This means that the differences in the performance of the LVQ classifiers are not significant and the null hypothesis is accepted.

DISCUSSION

The main data set used in this study is the brain MRI images which has been collected from UKM Medical Center, Malaysia. The images passed through different image enhancement techniques to remove noise and sharpen the edges, image segmentation and thresholding techniques, morphological operation and feature extraction techniques. Principle Component Analysis (PCA) is used to minimize the data set size by choosing only effective features vectors only.

LVQ algorithm invented by Kohonen (1988). These invented algorithms are used for training the nearest-neighbor classification. LVQ family consists of LVQ1, LVQ2 and the improved versions LVQ2.1, LVQ3, OLVQ1, OLVQ3, Multipass LVQ and HLVQ algorithms. LVQ algorithms are used for pattern classification, statistical pattern classification and signal processing.

The disadvantages of LVQ classifier are as follow (Grbovic and Vucetic, 2009):

- The classification results depend on the initial choice of prototypes. Choosing improper number of prototypes causes poor classification performance
- LVQ algorithms typically choose the same number of prototypes per class and the decision (chosen by user) there is no guarantee that the prototypes are going to adapt to the data in the best possible way. Some classes in multiclass datasets have complicated distribution in the feature space more than others. That means they get more number of prototypes. Also this leads to an issue when the class is highly unbalanced
- LVQ algorithms are not robust to noisy data and prototypes are sometimes trapped in the positions where they became useless

Prior to above statements and findings, Multi-pass LVQ outperforms other LVQ siblings as both methods uses the fast class distribution and optimization method for solving parameter tuning issue. On the other hand, Hierarchy LVQ puts a lot of attention in skipping overlap adjacent feature spaces when they appear close to the border of class separation.

In general, LVQ classifier assigns the input vectors to the code vectors by measuring the distance between them using Euclidean distance function. LVQ siblings algorithms were originally designed to tackle the problem that some neurons may win too often while others are always inactive, thus reducing the dependency on using training examples as initial weights. In these training examples, normally lack of all classes. Thus, multi randomization technique helps to improve the distribution of the training examples properly. To increase the chances of other neurons to be winners, rounding off function is applied to the Euclidean distance equation.

LVQ classifier has been discussed in this work. The results show that LVQ neural network classifier is a high performance classifier due to its simple structure which makes it faster than the back propagation networks; it can be used with normalized and not normalized input data, flexible which make applicable in general fields and the ability to recognize subclass. The factors that affect the LVQ classifier performance are the learning rate, number of the code vectors in the competitive layer and the initial weight. Many researchers such as Wang and Wen (2008) solved these problems by using Genetic algorithm to find the best LVQ NN initialization and features selection (Sasikala *et al*., 2006). The distance between the input vectors and the code vector is measured using Euclidian equation. Only the code vector with min distance will be the winner and the rest of code vector neurons will pushed away regardless if it contains important information or not.

CONCLUSION

In this study, some studies related to brain MRI segmentation and classification techniques are discussed. This study has demonstrated the possibility of using the supervised learning algorithm LVQ classifier for the brain tumor detection problem using MR images. The LVQ algorithm is effective at reducing large datasets, can manipulate dataset features andworks with datasets containing missing data. It can also be easily updated and applied to different problems. Thus, it is expected to achieve good results in detecting brain tumors from MR images using the LVQ classifier. The Multi pass LVQ showed better stability than the other LVQs and for that reason it has the great potential to be applied for brain imaging problems. In term of the performance accuracy rate, the ANOVA test showed no important difference between the LVQ siblings performance. Thus, with an appropriate image preprocessing techniques and with the correct dataset split percentage which includes all classes any version from LVQ siblings will be suitable to classify Brain MRI. However, the small size of the brain tumor dataset and the quality of the collected images could affect the classifiers performance.

For the future work a bigger size data set and different enhancement techniques to remove noise from images and improve the images homogeneity will be used to improve the classifiers performance.

ACKNOWLEDGMENTS

This study is based on two research grants from Ministry of Science, Technology and Innovation, Malaysia entitled "Science fund 01-01-02-SF0694 Spiking-LVQ Network For Brain Tumor Detection" and "FF-436-2011 Developing Diagnostic Imaging System for Brain Tumor". Many thanks to the CAIT researchers, such as Nurnaima Binti Zainuddin, for her help. Ethics approval entitled "FF-436-2011 Developing Diagnostic Imaging System for Brain Tumour" from UKM Medical Center, Malaysia for collecting and conducting experiments on MRI Brain Tumor patient's record was obtained.

REFERENCES

Abdullah, N., U.K. Ngah and S.A. Aziz, 2011. Image classification of brain MRI using support vector machine. Proceedings of the IEEE International Conference on Imaging Systems and Techniques, May 17-18, 2011, Penang, Malaysia, pp: 242-247.

Bache, K. and M. Lichman, 2013. UCI machine learning repository. University of California, School of Information and Computer Science, Irvine, CA. http://archive.ics.uci.edu/ml/citation_policy.html

Bataineh, B., S.N.H.S. Abdullah and K. Omar, 2012. A novel statistical feature extraction method for textual images: Optical font recognition. Expert Syst. Appli., 39: 5470-5477.

Chalabi, Z., N. Berrached, N. Kharchouche, Y. Ghellemallah, M. Mansour and H. Mouhadjer, 2008. Classification of the medical images by the kohonen network SOM and LVQ. J. Applied Sci., 8: 1149-1158.

Cherifi, D., M.Z. Doghmane, A. Nait-Ali, Z. Aici and S. Bouzelha, 2011. Abnormal tissus extraction in MRI brain medical images. Proceedings of the 7th International Workshop on Systems, Signal Processing and their Applications, May 9-11, 2011, Tipaza, Algeria, pp: 357-360.

Clausi, D.A., 2002. An analysis of co-occurrence texture statistics as a function of grey level quantization. Can. J. Remote Sens., 28: 45-62.

Coyne, K., 2012. MRI: A guided tour. http://www.magnet.fsu.edu/education/tutorials/magnetacademy/mri/fullarticle.html

Gaikwad, D.P., P. Abhang and P. Bedekar, 2011. Medical image segmentation for brain tumor detection. Proceedings of the International Conference and Workshop on Emerging Trends in Technology, Mumbai, Maharashtra, India, February 25-26, 2011, pp: 63-65.

Gopal, N.N. and M. Karnan, 2010. Diagnose brain tumor through MRI using image processing clustering algorithms such as Fuzzy C Means along with intelligent optimization techniques. Proceedings of the IEEE International Conference on Computational Intelligence and Computing Research, December 28-29, 2010, Coimbatore, India, pp: 1-4.

Grbovic, M. and S. Vucetic, 2009. Learning vector quantization with adaptive prototype addition and removal. Proceedings of the International Joint Conference on Neural Networks, June 14-19, 2009, Atlanta, GA., USA., pp: 994-1001.

Haralick, R.M., K. Shanmugam and I. Dinstein, 1973. Textural features for image classification. IEEE Trans. Syst. Man Cybernet., SMC-3: 610-621.

Hoffman, J.M., 2001. New advances in brain tumor imaging. Curr. Opin. Oncol., 13: 148-153.

Khuwaja, G.A., 2002. An adaptive combined classifier system for invariant face recognition. Digit. Signal Process., 12: 21-46.

Kirsch, E., B. Hammer and G. Von Arx, 2009. Graves orbitopathy: Current imaging procedures. Swiss Med. Wkly, 139: 618-623.

Kohonen, T., 1988. An introduction to neural computing. Neural Networks, 1: 3-16.

Lahmiri, S. and M. Boukadoum, 2011. Classification of brain MRI using the LH and HL wavelet transform sub-bands. Proceedings of the IEEE International Symposium on Circuits and Systems, May 15-18, 2011, Rio de Janeiro, Brazil, pp: 1025-1028.

MedlinePlus, 2012. Metastatic brain tumor. A Service of the U.S. National Library of Medicine National Institutes of Health. http://www.nlm.nih.gov/medlineplus/ency/article/000769.htm

Mingkun, Y., Y. Wei, Q. Xiangqian, Q. Jun, L. Zhenyang and F. Wenfeng, 2011. Imaging Techniques in Brain Tumor. In: Diagnostic Techniques and Surgical Management of Brain Tumors. Abujamra, A.L. (Ed.). InTech, China, ISBN: 978-953-307-589-1, pp: 43-66.

NCI, 2009. Tumor grades and types. National Cancer Institute (NCI). http://www.cancer.gov/cancertopics/wyntk/brain/page3

Otsu, N., 1979. A threshold selection method from gray-level histograms. IEEE Trans. Syst. Man Cybernet., 9: 62-69.

Pregenzer, M. and G. Pfurtscheller, 1995. Distinction sensitive learning vector quantization (DSLVQ)-application as a classifier based feature selection method for a brain computer interface. Proceedings of the 4th International Conference on Artificial Neural Networks, June 26-28, 1995, Cambridge, UK., pp: 433-436.

RajaRajan, A., 2011. Brain disorder detection using artificial neural network. Proceedings of the 3rd International Conference on Electronics Computer Technology, Volume 4, April 8-10, 2011, Kanyakumari, India, pp: 268-272.

Rajendran, P. and M. Madheswaran, 2009. An improved image mining technique for brain tumour classification using efficient classifier. Int. J. Comput. Sci. Inform. Secur., 6: 107-116.

Sasikala, M., N. Kumaravel and L. Subhashini, 2006. Automatic tumor segmentation using optimal texture features. Proceedings of the IET 3rd International Conference on Advances in Medical, Signal and Information Processing, July 17-19, 2006, Glasgow, UK., pp: 1-4.

Shubhangi, D.C. and P.S. Hiremath, 2009. Support vector machine (SVM) classifier for brain tumor detection. Proceedings of the International Conference on Advances in Computing, Communication and Control, January 23-24, 2009, Mumbai, Maharashtra, India, pp: 444-448.

Soh, L.K. and C. Tsatsoulis, 1999. Texture analysis of SAR sea ice imagery using gray level co-occurrence matrices. IEEE Trans. Geosci. Remote Sens., 37: 780-795.

USFDA, 2012. Radiation-emitting products. U.S. Food and Drug Administration. http://www.fda.gov/Radiation-EmittingProducts/RadiationEmittingProductsandProcedures/MedicalImaging/default.htm

Wang, J.M. and Y.Q. Wen, 2008. Application of genetic LVQ neural network in credit analysis of power customer. Proceedings of the 4th International Conference on Natural Computation, Volume 2, October 18-20, 2008, Jinan, China, pp: 305-309.

Xing, L. and D.T. Pham, 1995. Neural Networks for Identification, Prediction and Control. Springer-Verlag, New York, ISBN-13: 9783540199595.